THE ASTROPHYSICAL JOURNAL, 429:139–152, 1994 July 1

MAGNETICALLY DRIVEN JETS AND WINDS: EXACT SOLUTIONS

J. CONTOPOULOS[1]
Laboratory for High Energy Astrophysics, NASA/Goddard Space Flight Center, Greenbelt, MD 20771
AND
R. V. E. LOVELACE
Department of Applied Physics, Cornell University, Ithaca, NY 14853
Received 1993 September 27; accepted 1993 December 29

ABSTRACT

We present a general class of self-similar solutions of the full set of MHD equations that include matter flow, electromagnetic fields, pressure, and gravity. The solutions represent axisymmetric, time-independent, nonrelativistic, ideal, magnetohydrodynamic, collimated outflows (jets and winds) from magnetized accretion disks around compact objects. The magnetic field extracts angular momentum from the disk, accelerates the outflows perpendicular to the disk, and provides collimation at large distances. The terminal outflow velocities are of the order of or greater than the rotational velocity of the disk at the base of the flow. When a nonzero electric current flows along the jet, the outflow radius oscillates with axial distance, whereas when the total electric current is zero (with the return current flowing across the jet's cross section), the outflow radius increases to a maximum and then decreases. The method can also be applied to relativistic outflows.

Subject headings: galaxies: jets — ISM: jets and outflows — MHD — stars: mass loss

1. INTRODUCTION

Bipolar outflows in galactic (protostars) and extragalactic (active galactic nuclei) environments seem to be associated with mass accretion into a central compact object. Theoretical models involve various physical mechanisms which power and collimate the outflows (nozzles, funnels, winds, magnetic fields; see Begelman, Blandford, & Rees 1984, for a review). We favor magnetodynamic mechanisms for the following reasons:

1. The continuum radiation from jets (radio, optical, X-ray) is believed to be optically thin synchrotron, from electrons of energies ~ 100 MeV–10 GeV, spiralling along magnetic field lines $\sim 10^{-6}$–10^{-1} G. Polarization measurements often show high degrees of polarization ($\sim 60\%$, close to the theoretical maximum of 70% for synchrotron radiation), which suggests that the magnetic field is organized on a large scale. The $\boldsymbol{B}$ field may also have small-scale fluctuations. Polarization measurements of bright knots and hot spots suggests magnetic field orientation perpendicular to the jet direction, which agrees with the interpretation of hot spots as shocks and as regions of particle reacceleration (e.g., Hughes, Aller, & Aller 1985, 1989a, b; for VLBI polarization measurements see Wardle & Roberts 1988).

2. The high collimations observed in some sources (e.g., NGC 6251), and the evidence for continuing collimation in extragalactic (FR I) and galactic sources (e.g., Mundt, Ray, & Raga 1991), makes mechanisms that involve initial precollimation (funnels) and intergalactic ram pressure confinement unlikely.

3. N-body simulations of Alfvén wave effects in self-gravitating clouds (Pudritz 1988) suggest that magnetic fields of energy densities comparable to gravitational energy play a role in producing the filamentary structure observed in galactic molecular clouds (e.g., Bally et al. 1987; Ungerechts & Thaddeus 1987).

4. Magnetic fields "frozen" into ionized accreting material are very efficient in extracting angular momentum and, thus, slowing down protostars (e.g., Weber & Davis 1967; Mouschovias & Paleologou 1980; Pudritz 1985). On the other hand, thermally or radiatively driven winds have an angular momentum per unit mass equal to that of the accreting matter.

The main objective of the present work is to develop time-independent *magnetically driven* and *collimated* outflows. We do not discuss secondary questions, such as the reacceleration mechanisms of particles within the jets, the role of shocks and instabilities, and the role of turbulence and viscosity in shearing the magnetic field. These topics are reviewed by Begelman et al. (1984) and Hughes (1991).

Previous studies of magnetohydrodynamic (MHD) jets and winds have obtained estimates of the parameters of the outflows (rates of mass, energy and angular momentum flow, average flow velocity, magnetic field configurations, etc.) without obtaining fully self-consistent solutions (e.g., Koupelis & Van Horn 1989; Lovelace, Berk, & Contopoulos 1991, hereafter LBC). This is because of the nonlinearity of the equations and the complications associated with critical and singular points. However, numerical solutions have been obtained for both the nonrelativistic (Sakurai 1985) and relativistic regimes (Camenzind 1987). Here we present quasi-analytic self-similar self-consistent solutions to the full set of *ideal, time-independent, axisymmetric, nonrelativistic* MHD equations which describe outflows from a thin disk accreting into a central compact object. Quasi-analytic solutions of the full set of equations have been obtained previously by Blandford & Payne (1982, hereafter BP), Tsinganos & Trussoni (1990), Tsinganos & Sauty (1993), and others.

[1] NAS/NRC Resident Research Associate.

The present work is a generalization of BP's self-similar results, although we have followed a different approach in that we use the formalism of the generalized Grad-Shafranov equation. In § 2 of this paper we derive the basic equations of our theory. We discuss the physics and methods of solutions in § 3, and in § 4 we compare our analysis to the BP limit. Our main results are summarized in § 5. The relativistic equations are presented in the Appendix.

2. THEORY

2.1. *Basic Equations*

We follow the formalism of Lovelace et al. (1986, hereafter LMMS). In § 4, we will make the comparison with BP's notation.

Let us consider a thin ionized accretion disk around a central compact object. The disk is threaded by a magnetic field, and outflows of matter leave the top and bottom surfaces of the disk. The outflows are considered to be axisymmetric ($\partial/\partial\phi = 0$), stationary ($\partial/\partial t = 0$), nondissipative, and nonrelativistic (the relativistic case is discussed in the Appendix). Nonideal effects (Ohmic diffusivity, ambipolar diffusion—the drift of ionized particles to which the magnetic field is frozen, relative to the neutrals) are most likely to be important only in the *interior* of the accretion disk (see Lovelace, Wang, & Sulkanen 1987; Königl 1989; Wang, Sulkanen, & Lovelace 1992; etc.). We use a cylindrical, inertial coordinate system (r, ϕ, z) with the origin fixed on the central object and the z-axis perpendicular to the disk. The accretion disk (at $z = 0$) rotates counterclockwise and "drags" the magnetic field lines backward, into a more and more toroidal configuration (B_ϕ) at larger distances. The matter flow rotates with the disk initially, but becomes more and more axial farther out (see Fig. 1 of LBC).

Thus, following LMMS, the basic equations of our problem are those of ideal nonrelativistic MHD that include pressure and gravity:

$$\nabla \cdot (\rho \boldsymbol{v}) = 0 , \tag{1}$$

$$\nabla \times \boldsymbol{B} = \frac{4\pi}{c} \boldsymbol{J} , \tag{2}$$

$$\boldsymbol{E} + \frac{1}{c} \boldsymbol{v} \times \boldsymbol{B} = 0 , \tag{3}$$

$$\nabla \times \boldsymbol{E} = 0 , \tag{4}$$

$$\rho(\boldsymbol{v} \cdot \nabla)\boldsymbol{v} = -\nabla p + \rho \boldsymbol{g} + \frac{1}{c} \boldsymbol{J} \times \boldsymbol{B} , \tag{5}$$

$$\nabla \cdot \boldsymbol{B} = 0 , \tag{6}$$

where $\boldsymbol{v}$ is the flow velocity, $\boldsymbol{E}$ and $\boldsymbol{B}$ are the electric and magnetic field, respectively, $\boldsymbol{J}$ is the electric current, p is the pressure, ρ is the matter density, and $\boldsymbol{g}$ is the gravitational force per unit mass. In order to "close" the above system of equations we also need an equation of state to relate the pressure and the density. In what follows we assume for simplicity that the flow is adiabatic. We note that more complicated equations of state have been used (e.g., outflows that start out isothermally and become isentropic; Parker 1963). Some people even consider the use of a polytropic equation of state too restrictive and prefer to specify a priori the form of the outflow streamlines (e.g., Tsinganos & Trussoni 1990).

Owing to the axisymmetry, the magnetic field can be separated into *poloidal* and *toroidal* parts:

$$\boldsymbol{B} = \boldsymbol{B}_p + \boldsymbol{B}_\phi , \tag{7}$$

with

$$\boldsymbol{B}_p = \frac{1}{r} \nabla\Psi \times \hat{\boldsymbol{\phi}} , \tag{8}$$

where $\Psi(r, z)$ is the magnetic flux function. The lines of constant $\Psi(r, z)$ in the r-z plane are the poloidal projections of the field lines.

When we solve the above system of equations we obtain a set of quantities conserved along flux surfaces. These quantities (the functions F, Ω, H, J, and S of Ψ, defined below) are connected to the boundary conditions on the disk (at $z = 0$). Following LMMS, the continuity equation (1) and $\nabla \cdot \boldsymbol{B} = 0$ imply

$$4\pi\rho \frac{|\boldsymbol{v}_p|}{|\boldsymbol{B}_p|} = F(\Psi) , \tag{9}$$

which, together with equations (3) and (4), implies that

$$\boldsymbol{v} = r\Omega(\Psi)\hat{\boldsymbol{\phi}} + \frac{F(\Psi)}{4\pi\rho} \boldsymbol{B} . \tag{10}$$

We note here that $\boldsymbol{v}$ is in general *not* parallel to $\boldsymbol{B}$ (according to Jackson 1975, the field lines "frozen-into" the fluid drift with a velocity $c(\boldsymbol{E} \times \boldsymbol{B})/B^2 = (\boldsymbol{B} \times \boldsymbol{v}) \times \boldsymbol{B}/B^2 = r\Omega(\boldsymbol{B}_p \times \hat{\boldsymbol{\phi}}) \times \boldsymbol{B}/B^2$, which is equal to the component of $\boldsymbol{v}$ perpendicular to $\boldsymbol{B}$). We will come back to this in § 4, when we discuss the magnetic driving of the outflow.

Conservation of angular momentum flow on each flux surface gives

$$-F(\Psi)rv_\phi + rB_\phi = H(\Psi)\,. \tag{11}$$

The Bernoulli equation (energy flow conservation) now becomes

$$\int (d\rho/\rho)\Big|_{\Psi=\text{const.}} + \tfrac{1}{2}|\boldsymbol{v}|^2 + \Phi_g - rv_\phi\Omega(\Psi) = J(\Psi)\,, \tag{12}$$

which includes the enthalpy, matter flow, gravity, and Poynting flux $-r\Omega B_\phi/F = -r\Omega v_\phi - \Omega H/F$ (the $-\Omega H/F$ term is a function of Ψ and is included in $J(\Psi)$). We assume for simplicity that the flow is adiabatic; that is,

$$S(p,\rho) = k_B(\Gamma-1)^{-1}\ln(p/\rho^\Gamma) = S(\Psi)\,, \tag{13}$$

where S is the entropy per unit volume of the flow. Here k_B is the Boltzmann constant, and Γ is the usual specific heat ratio (adiabatic index). Finally, the poloidal component of the force balance equation (5) perpendicular to the flux surfaces (i.e., parallel to $\nabla\Psi$), gives the *generalized, nonrelativistic Grad-Shafranov equation* for $\Psi(r, z)$ (LMMS):

$$\left(1-\frac{F^2}{4\pi\rho}\right)\Delta^*\Psi - F\nabla\left(\frac{F}{4\pi\rho}\right)\cdot\nabla\Psi = -4\pi\rho r^2(J' + rv_\phi\Omega') - (H + rv_\phi F)(H' + rv_\phi F') + 4\pi r^2 p(S'/k_B)\,, \tag{14}$$

where

$$\Delta^* \equiv r\frac{\partial}{\partial r}\frac{1}{r}\frac{\partial}{\partial r} + \frac{\partial^2}{\partial z^2}\,,$$

and primes denote differentiation with respect to Ψ. Flow and magnetic field lines lie along $\Psi(r, z) = $ const. magnetic flux surfaces. We emphasize that a solution to the Grad-Shafranov equation (14) for a given set of functions F, Ω, H, J, and S, is equivalent to a solution of the full set of basic equations, (1)–(6).

Equation (14) is a second-order partial differential equation of mixed type (Heinemann & Olbert 1978; LMMS), and the flow field is in general separated by three critical surfaces which are not known a priori (they are obtained along with the solution for Ψ). The different regimes of the Grad-Shafranov equation are:

1. Elliptic for $v_p^2 < v_c^2$,
2. Hyperbolic for $v_c^2 < v_p^2 < v_{\rm sms}^2$,
3. Elliptic for $v_{\rm sms}^2 < v_p^2 < v_{\rm fms}^2$, and
4. Hyperbolic for $v_{\rm fms}^2 < v_p^2$.

Here $v_p \equiv (v_z^2 + v_r^2)^{1/2}$ is the poloidal flow velocity; $v_c \equiv c_s v_{\rm Ap}/(c_s^2 + v_{\rm A}^2)^{1/2}$ is the speed of the cusp of the slow-mode wave front; $v_{\rm sms,fms} \equiv (1/2\{c_s^2 + v_{\rm A}^2 \pm [(c_s^2 + v_{\rm A}^2)^2 - 4c_s^2 v_{\rm Ap}^2]^{1/2}\})^{1/2}$ are the slow and fast magnetosonic speeds, respectively; $c_s \equiv (\partial p/\partial\rho)_S^{1/2}$ is the adiabatic speed of sound; $v_{\rm Ap} \equiv |\boldsymbol{B}_p|/(4\pi\rho)^{1/2}$ is the poloidal Alfvén speed; and $v_{\rm A} \equiv |\boldsymbol{B}|/(4\pi\rho)^{1/2}$ is the total Alfvén speed. Therefore, since the techniques of integration of elliptic equations are different from the techniques of integration of hyperbolic ones, the numerical solution of equation (14) presents a computational challenge.

2.2. *Renormalizations*

Our goal is to solve equation (14) analytically. We do this by transforming it, from a *partial*, to an *ordinary* differential equation. The method that is presented here simplifies the problem considerably by using special boundary conditions and special renormalizations of parameters; it reproduces however the interesting known characteristics of collimated outflows.

We first nondimensional r and z by redefining them as

$$r/a_i \quad \text{and} \quad z/a_i\,, \tag{15}$$

where a_i is a "characteristic" jet radius (this was identified as the initial jet radius in the solution of LBC; here it is more general). As in BP, we assume a self-similar scaling (however, following the formalism of the generalized Grad-Shafranov equation and our experience from LBC, we are able to consider a much wider class of boundary conditions on the disk). The main idea has been the following: time-independent axisymmetric magnetic field configurations are characterized by a set of nested magnetic flux surfaces $\Psi(r, z) = $ const. In our case of jet configuration, there is a one-to-one correspondence between the value of Ψ and the distance r_Ψ at which the flux surface intersects the plane of the disk; the general equation for the flux surface is of the form $r = r_\Psi R(z; r_\Psi)$, where $R(0; r_\Psi) = 1$. We simplify the problem by looking for self-similar solutions of the form

$$r = r_\Psi R(z/r_\Psi) \equiv r_\Psi R(Z)\,, \tag{16}$$

where $Z \equiv z/r_\Psi$ is the renormalized z variable. The above scaling and a suitable choice of boundary conditions along the disk enable us to separate the r_Ψ dependence from the Z dependence of our equations and to reduce the problem to the numerical solution of an ordinary second-order differential equation. Note that in LBC, we made use of the Ansatz that $\Psi(r, z) = \Psi(r/R(z))$, or equivalently, $r = r_\Psi R(z)$, which does not give a fully self-consistent solution.

Consider next the form of the relation between $\Psi(r, z)$ and r_Ψ. We would like to be able to rescale the r_Ψ terms in our equations, and in order to do it, Ψ *must* have a simple power-law dependence on r_Ψ,

$$\Psi(r, z) = (r_\Psi)^x\Psi_0\,, \tag{17}$$

where x is a free exponent, and $\Psi_0 = \text{const}$. Consequently, the magnetic field scales as

$$\boldsymbol{B}(r, z) = (r_\Psi)^{x-2}\boldsymbol{B}(Z) . \tag{18}$$

Thus, the free exponent x controls the initial field profile. At $z = 0$, $\boldsymbol{B}(r, 0) \propto r^{x-2}$. Note that in BP's special solution the magnetic field is taken to scale as $r^{-5/4}$, which is equivalent to $x = 3/4$. Note also that for $x < 1$ the total axial electric current flowing into the disk within a distance ra_i, $I = 2\pi c(ra_i)B_\phi(r, z = 0) \propto r^{x-1}$, has a double singularity at small radii. We will come back to this in § 5.

Next, consider the Euler equation. The gravitational force term $\boldsymbol{g}$ scales as $(r_\Psi)^{-2}$, and because the ∇ terms scale as $(r_\Psi)^{-1}$, we choose

$$\boldsymbol{v}(r, z) = (r_\Psi)^{-1/2}\boldsymbol{V}(Z)v_0 , \tag{19}$$

where v_0 is the initial rotational velocity at the characteristic radius, and $V(z)$ is dimensionless. Note that this corresponds to a "Keplerian-like" rotational profile, although $v_\phi(r, 0)$ can be different (but proportional to) $v_K(r)$. The Bernoulli constant $J(\Psi)$ scales as $\boldsymbol{v}^2$, so that

$$J(\Psi) = (r_\Psi)^{-1}J_0 v_0^2 . \tag{20}$$

The constant $\Omega(\Psi)$ scales as v_ϕ/r, so that

$$\Omega(\Psi) = (r_\Psi)^{-3/2}\Omega_0 \frac{v_0}{a_i} . \tag{21}$$

The constant $H(\Psi)$ scales as rB_ϕ, so that

$$H(\Psi) = (r_\Psi)^{x-1}H_0 a_i B_0 . \tag{22}$$

$F(\Psi)$ scales as $H(\Psi)/(rv_\phi)$, so that

$$F(\Psi) = (r_\Psi)^{x-3/2}F_0 \frac{B_0}{v_0} , \tag{23}$$

where, $B_0 = B_z(Z = 0)$. We consider finally the density and pressure terms. Using equation (9) and the above results, we obtain

$$\rho(r, z) = (r_\Psi)^{2x-3}\rho(Z) \frac{B_0^2}{v_0^2} . \tag{24}$$

The pressure must then scale as

$$p(r, z) = (r_\Psi)^{2x-4}p(Z)B_0^2 . \tag{25}$$

We will assume that the flow of matter is adiabatic for simplicity; hence, according to equation (13),

$$S(\Psi) = k_B(\Gamma - 1)^{-1}\{[(2x - 4) - \Gamma(2x - 3)] \ln r_\Psi + \ln \mathcal{K}\} , \tag{26}$$

where $p(Z) = \mathcal{K}\rho(Z)^\Gamma$, and $\mathcal{K}$ is a dimensionless constant. Note that the adiabatic speed of sound is

$$c_s \equiv \left[\left(\frac{\partial p}{\partial \rho}\right)_S\right]^{1/2} = (r_\Psi)^{-1/2}[\mathcal{K}\Gamma\rho(Z)^{\Gamma-1}]^{1/2}v_0 \equiv (r_\Psi)^{-1/2}C_s(Z)v_0 . \tag{27}$$

The quantities V, ρ, p, C_s, J_0, Ω_0, H_0, and F_0 are dimensionless.

2.3. *The Renormalized Equation*

We now show that, using the expressions of § 2.2, the Grad-Shafranov equation (14) is reduced into one ordinary differential equation of second order for $R(Z)$ in terms of the renormalized variable $Z \equiv z/r_\Psi$. As in our earlier work (LBC), we reduce the MHD equations to the problem of obtaining the form of one field line, $r = R(z)$. However, we now obtain the full solution for the flow and the fields in the entire poloidal r-z plane (as shown in Fig. 1). The different quantities are given by equations (16)–(27).

Care is needed in taking derivatives with respect to "unnormalized" variables because they depend on the parameter r_Ψ. As one moves away from a given point in the r-z plane, the nearby field lines have different values of r_Ψ. It is easily shown that

$$\left.\frac{\partial r_\Psi}{\partial r}\right|_z \equiv (r_\Psi)_r = \frac{1}{R - ZR'} , \tag{28}$$

$$\left.\frac{\partial r_\Psi}{\partial z}\right|_r \equiv (r_\Psi)_z = -\frac{R'}{R - ZR'} , \tag{29}$$

and hence that

$$\left.\frac{\partial}{\partial r}Z\right|_z \equiv Z_r = -\frac{1}{r_\Psi}\frac{Z}{R - ZR'} , \tag{30}$$

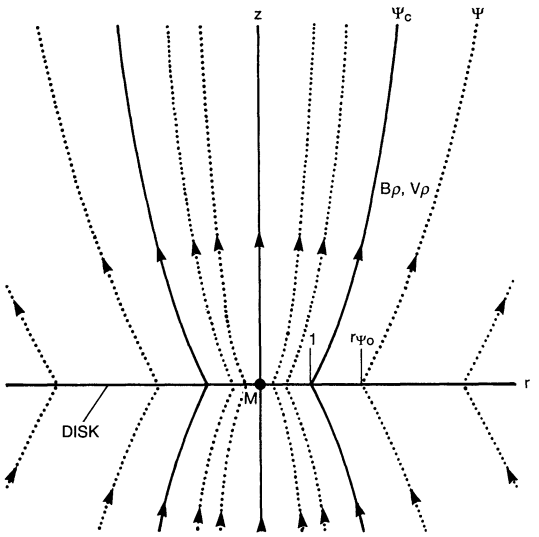

FIG. 1.—Poloidal r-z plane. The thick line represents the solution $r = R(z)$, with $R(z = 0) = 1$. A general field line characterized by $\Psi(r, z) = \text{const}$, which originates at $r_{\Psi 0}$, is given by $r = r_{\Psi 0} R(z/r_{\Psi 0})$. The values of the other flow parameters along that field line are given by eqs. (16)–(27). For the "even" solution shown here, $v_p \parallel B_p$ for $z > 0$, and $v_p \parallel -B_p$ for $z < 0$.

$$\left.\frac{\partial}{\partial z} Z\right|_r \equiv Z_z = \frac{1}{r_\Psi} \frac{R}{R - ZR'}, \tag{31}$$

$$\left.\frac{\partial^2}{\partial r^2} r_\Psi\right|_z \equiv (r_\Psi)_{rr} = -\frac{1}{r_\Psi} \frac{Z^2 R''}{(R - ZR')^3}, \tag{32}$$

$$\left.\frac{\partial^2}{\partial z^2} r_\Psi\right|_r \equiv (r_\Psi)_{zz} = -\frac{1}{r_\Psi} \frac{R^2 R''}{(R - ZR')^3}, \tag{33}$$

where $R' = dR/dZ$, and $R'' = d^2R/dZ^2$. Thus, using equations (8) and (10), the magnetic field components are given by

$$B_r(r, z) = (r_\Psi)^{x-2} \frac{R'}{R(R - ZR')} B_0, \tag{34}$$

$$B_\phi(r, z) = (r_\Psi)^{x-2} \frac{1}{R} \frac{H_0 + F_0 \Omega_0 R^2}{1 - F_0 V_z R(R - ZR')} B_0, \tag{35}$$

$$B_z(r, z) = (r_\Psi)^{x-2} \frac{1}{R(R - ZR')} B_0, \tag{36}$$

where $B_0 \equiv x\Psi_0/a_i^2$. Taking into account that $4\pi\rho = FB_z/v_z$ and factoring out the $(r_\Psi)^{x-2} B_0$ terms, the Grad-Shafranov equation (14) can be written as

$$\begin{aligned}
&[1 - F_0 V_z R(R - ZR')]\left[-\frac{(r_\Psi)_r}{R} + (x - 1)((r_\Psi)_r^2 + (r_\Psi)_z^2) + ((r_\Psi)_{rr} + (r_\Psi)_{zz}) r_\Psi \right] - F_0 \left[\left(\frac{V_z R}{(r_\Psi)_r} \right)' (Z_r (r_\Psi)_r + Z_z (r_\Psi)_z) r_\Psi \right. \\
&\qquad \left. + \left(-x + \frac{3}{2} \right) \frac{V_z R}{(r_\Psi)_r} ((r_\Psi)_r^2 + (r_\Psi)_z^2) \right] = -F_0 \frac{(r_\Psi)_r}{V_z R} R^2 \left[-J_0 + R V_\phi \left(-\frac{3}{2} \Omega_0 \right) \right] \\
&\qquad -(H_0 + R V_\phi F_0) \left[(x - 1) H_0 + R V_\phi \left(x - \frac{3}{2} \right) F_0 \right] + 4\pi R^2 C_s^2 \left(\frac{F_0}{4\pi} \frac{(r_\Psi)_r}{R V_z} \right) \frac{(2x - 4) - \Gamma(2x - 3)}{\Gamma(\Gamma - 1)},
\end{aligned} \tag{37}$$

where primes denote differentiation with respect to Z,

$$C_s^2 = \mathcal{K} \Gamma \left(\frac{F_0}{4\pi} \frac{(r_\Psi)_r}{R V_z} \right)^{\Gamma - 1}, \tag{38}$$

and

$$V_\phi = \frac{R\Omega_0 + H_0 V_z (R - ZR')}{1 - F_0 V_z R(R - ZR')}. \tag{39}$$

The Bernoulli equation (12) gives

$$\frac{1}{\Gamma-1}(C_s^2-C_{s0}^2)+\frac{V_z^2}{2}(1+(R')^2)+\frac{1}{2}V_\phi^2+\frac{\Phi_g}{v_0^2}-RV_\phi\Omega_0=J_0\,, \tag{40}$$

where $C_{s0}^2=C_s^2(Z=0)\equiv\mathcal{K}\Gamma[F_0/4\pi V_z(Z=0)]^{\Gamma-1}$, and $\Phi_g=-(GM/a_i)[1/(R^2+Z^2)^{1/2}]$. We will root-solve equation (40) to get V_z as a function of R, R', and Z. Differentiating this equation with respect to Z gives

$$V_z'=\mathcal{A}+\mathcal{B}R''\,, \tag{41}$$

where

$$\mathcal{A}(R,R',Z)\equiv\frac{\mathcal{C}}{\mathcal{E}}(R,R',Z)\,,\qquad \mathcal{B}(R,R',Z)\equiv\frac{\mathcal{D}}{\mathcal{E}}(R,R',Z)\,,$$

and

$$\mathcal{C}(R,R',Z)\equiv-\left(-C_s^2\frac{R'}{R}+\frac{\Phi_g'}{v_0^2}-R'V_\phi\Omega_0\right)\frac{[1-F_0V_zR(R-ZR')]^2}{V_z(R-ZR')(H_0+\Omega_0F_0R^2)}-[R'\Omega_0+V_\phi F_0V_zR'(R-ZR')]\,,$$

$$\mathcal{D}(R,R',Z)\equiv-\left(C_s^2\frac{Z}{R-ZR'}+V_z^2R'\right)\frac{[1-F_0V_zR(R-ZR')]^2}{V_z(R-ZR')(H_0+\Omega_0F_0R^2)}+H_0V_zZ+V_\phi F_0V_zZR\,,$$

$$\mathcal{E}(R,R',Z)\equiv\left[-C_s^2\frac{1}{V_z}+V_z(1+(R')^2)\right]\frac{[1-F_0V_zR(R-ZR')]^2}{V_z(R-ZR')(H_0+\Omega_0F_0R^2)}+H_0(R-ZR')+V_\phi F_0R(R-ZR')\,.$$

We can finally put everything back into the Grad-Shafranov equation (14) and thereby obtain an expression for R'' as a function of R, R', and Z:

$$R''=\frac{\mathcal{F}}{\mathcal{G}}(R,R',Z)\,, \tag{42}$$

where

$$\begin{aligned}\mathcal{F}(R,R',Z)=&-[1-F_0V_zR(R-ZR')]\left[-\frac{1}{R(R-ZR')}+(x-1)\frac{1+(R')^2}{(R-ZR')^2}\right]\\&+F_0\left\{-\frac{Z+RR'}{(R-ZR')^2}[\mathcal{A}R(R-ZR')+V_zR'(R-ZR')]+V_zR(R-ZR')\left(\frac{3}{2}-x\right)\frac{1+(R')^2}{(R-ZR')^2}\right\}\\&+F_0\frac{R}{V_z(R-ZR')}\left(J_0+RV_\phi\frac{3}{2}\Omega_0\right)-(H_0+RV_\phi F_0)\left[(x-1)H_0+RV_\phi\left(x-\frac{3}{2}\right)F_0\right]\\&+4\pi R^2C_s^2\left[\frac{F_0}{4\pi}\frac{1}{V_zR(R-ZR')}\right]\frac{(2x-4)-\Gamma(2x-3)}{\Gamma(\Gamma-1)}\,,\end{aligned}$$

and

$$\mathcal{G}(R,R',Z)=[1-F_0V_zR(R-ZR')]\left[-\frac{R^2+Z^2}{(R-ZR')^3}\right]+F_0\frac{Z+RR'}{(R-ZR')^2}[\mathcal{B}R(R-ZR')-V_zRZ]\,.$$

Equation (42) is the final second-order ordinary differential equation for $R(Z)$, where V_z as a function of R, R', and Z is given by equation (40). We note again that equation (14) is *the* most general equation of axisymmetric ideal MHD flows which include fluid pressure and gravity. In the present work, we concentrate on collimated magnetized matter outflows from thin accretion disks.

3. SOLUTION AND DISCUSSION

The physical situation is the following: Within the disk, the flow velocity is mainly azimuthal, $\boldsymbol{v}(r=a_i,z=0)\approx v_0\hat{\boldsymbol{\phi}}$, but there is also a small flow out of the disk plane ($v_z(r=a_i,z=0)=V_{z0}v_0\ll v_0$). Our definition of v_0 as the initial rotational velocity at the characteristic radius a_i implies that $V_\phi(Z=0)=(\Omega_0+H_0V_{z0})/(1-F_0V_{z0})=1$; hence

$$\Omega_0=1-(F_0+H_0)V_{z0}\,. \tag{43}$$

Therefore, we integrate equation (42) numerically from $Z=0$, with the "initial" conditions $R(Z=0)=1$ and $R'(Z=0)\equiv R_0'$, a free parameter determined by the condition that the flow goes smoothly through the Alfvén singular point. We do not solve for the initial acceleration through the cusp and slow magnetosonic critical points and will simply start the integration with $V_{z0}>V_{\rm sms}$. The reason is the following: Consider the first-order term of the expansion of equation (40) near $Z=0$,

$$C_{s0}^2\left(-\frac{V_0'}{V_0}-R_0'\right)+V_0V_0'(1+(R_0')^2)+V_0^2R_0'R_0''+\delta_0R_0'-R_0'\Omega_0=0\,, \tag{44}$$

where $\delta_0 \equiv v_K^2/v_0^2$, and v_K is the Keplerian velocity at the characteristic radius a_i (in our notation $\Phi_g \equiv -\delta_0 v_0^2(R^2 + Z^2)^{-1/2}$). Note that BP have $\delta_0 = 1$; this is however very restrictive, and more recent work has $\delta_0 \neq 1$ (Lovelace et al. 1987; Königl 1989; LBC).

We see that when $V_0 \approx 0$, the pressure gradient term is the most important factor that controls the evolution of the outflow. Therefore, for $V_{z0} \leq C_{s0} \approx V_{sms} \ll V_{Ap}$, the problem is almost purely hydrodynamical, and the initial acceleration involves a "de Laval nozzle"–type sub/supersonic transition very close to the origin of the outflow. Our equations include pressure and reduce to a "solar-wind"–type outflow in the absence of magnetic fields. However, it is precisely the effect of the magnetic field in accelerating the flow outward that we are interested in, and therefore, we consider situations where the fluid pressure is a secondary contribution. BP neglect pressure altogether and start with $V_{z0} = 0$ (but $(\rho V_z)_0$ finite).

For $V_z > V_{sms}$, the important driving mechanism which counteracts gravity is the gradient of the effective magnetic field pressure. In order to understand this, let us consider again equation (10). We see here that in general (i.e., when $\Omega(\Psi) \neq 0$) $\boldsymbol{v}$ *is not parallel to* $\boldsymbol{B}$, although we tend to think that in ideal (infinite conductivity) MHD, the matter flows *along* the field lines. The physical picture is the following: magnetic field lines act like rotating spiral solid wires (along Ψ = const. flux surfaces) that confine beads moving freely among them. The important point is that each surface of wires rotates rigidly with angular velocity $\Omega(\Psi)$. In other words, the ionized disk to which the magnetic field lines are anchored imposes a rigid body rotation to each magnetic flux surface Ψ = const. Note however that $v_\phi = r\Omega$ *only* when $B_\phi = 0$. It is now easy to understand why rotating spiral magnetic field lines can accelerate a flow outward only when the direction of magnetic field winding is opposite to the direction of rotation (i.e., v_ϕ and B_ϕ have opposite signs, for $z > 0$). Needless to say that the exact geometry of rotating field lines is obtained as a solution of the full set of MHD equations which include matter flow.

BP consider purely poloidal rigid wires in their analogy (p. 885 of their paper) and conclude that the winds are centrifugally driven. However, once a fluid element moves out of the plane of the disk, the magnetic field is not only poloidal anymore, and it is precisely the "winding" of the field lines which produces collimation and axial acceleration: the analogy with the rotating rigid wires holds at all distances (this point is not emphasized in the literature). Another way to look at it is that the rotation of the ionized disk (to which the field lines are anchored) is indeed the prime mover of the rotating magnetosphere; however, it is the tension of the magnetic field lines which "mediates" this rotation at all distances. Therefore, we prefer to think that the jets are magnetically (and not centrifugally) driven.

The Alfvén point is not a critical point, since the Grad-Shafranov equation remains elliptical as V_p increases through V_{Ap}. Nevertheless, it is a zero of the denominator of our main equation and, therefore, an important singular point. We have argued that the important driving mechanism is the magnetic field. Therefore, the outflows start with a small velocity out of the disk plane, and as the flow moves away from the disk, energy is transferred from the electromagnetic field to the matter. In other words, the ratio of poloidal kinetic energy density to poloidal magnetic energy density is initially small, $\frac{1}{2}\rho v_p^2/(B_p^2/8\pi) \equiv M_{Ap}^2 < 1$ (M_{Ap} is the poloidal Alfvén Mach number), whereas at large distances it is large, $M_{Ap}^2 > 1$. Hence, a physical outflow solution goes smoothly through the Alfvén point at some finite distance. This last requirement determines the initial opening angle, or $R'(Z = 0)$. In general, we find a unique value of $R'(Z = 0) \equiv R_0'$.

By analogy to the de Laval nozzle or the solar wind problem, we see here a deep connection between the transition through a singular point and the acceleration mechanism of the flow: it is the gradient of the fluid (magnetic field) pressure which accelerates the one special solution through the sonic (Alfvén) singular point. We see this explicitly in equation (40): the term which counteracts gravity is the last term of the left-hand side, $-R\Omega(\Psi)V_\phi$, which, as we said, is the Poynting flux contribution to the energy flux.

With increasing distance Z, the jet's radius increases to a maximum value and then begins to decrease. We can see this by comparing the different terms in the radial force balance equation. At large distances, the "centrifugal" term

$$-\rho \frac{v_\phi^2}{r} \approx \frac{(\Omega_0 + H_0 V_z)^2}{4\pi V_z^3 F_0} \frac{(r_\Psi)^{2x-5}}{R^5} \frac{B_0^2}{a_i} \tag{45}$$

is balanced by the "magnetic force" term

$$\frac{1}{4\pi} \frac{B_\phi^2}{r} + \frac{1}{8\pi} \frac{\partial B_\phi^2}{\partial r} \approx \frac{\Omega_0^2}{4\pi V_z^2} (x - 1 - Z^2 R'') \frac{(r_\Psi)^{2x-5}}{R^3} \frac{B_0^2}{a_i}, \tag{46}$$

which is the sum of the pressure $(1/4\pi)B_\phi^2/r$ and the tension $(1/8\pi)\,\partial B_\phi^2/\partial r$. It is easily seen that when the jet radius R becomes large enough, the magnetic term becomes more important, and "the centrifugal force cannot support the jet against constriction by the magnetic tension" (BP, p. 892). When $x > 1$, the magnetic tension is always inward ($\propto (x - 1)B_\phi^2/r$) and the flow recollimates at relatively small axial distances. This is expected since, for $x > 1$, the jet carries a nonzero axial current. The larger the value of x, the larger the current, and thus the stronger the recollimation effect. On the other hand, when $x < 1$, the magnetic force is initially *outward*, the flow reaches large distances, and the term $-Z^2R''$ becomes important in recollimating the flow. As x approaches unity, the recollimation distances approach infinity. In Table 1 we can see how the axial distances of maximum radius vary, as we vary x, for a representative choice of jet parameters.

The jet evolution at very large distances beyond the distance of maximum of R also depends on the value of the exponent x. When $x < 1$, the magnetic field is almost purely toroidal, and at some very large distance the flow is chocked. BP suggest that the introduction of some extra internal pressure (e.g., through reheating during the recollimation phase), or the addition of external pressure, will help the flow "survive" the collapse and "bounce," as obtained in Chan & Henriksen (1980) and LBC. However, the flow is chocked *not* because the radius becomes extremely small (in that case, rotation would prevent the collapse), but because it turns around toward the symmetry axis (i.e., $R' \to -\infty$). Therefore, pressure might never be important, and it is probably the assumption of steady state which breaks down at those distances. When $x > 1$, rotation is sufficient to hold the collapse, and the jet evolves smoothly through a series of recollimations and bounces at logarithmically equal distances. BP have $x = 3/4 < 1$; therefore,

TABLE 1

LONG-RANGE BEHAVIOR OF A REPRESENTATIVE SOLUTION FOR VARIOUS VALUES OF x

x	R'_0	Z_{fms}	Z_{max}	R_{max}	V_{zmax}
0.5	3.5	3.5	67	28.5	5.9
0.7	2.42	8.3	353	73	6.0
0.75	2.18	11.3	3980	188	6.0
0.8	1.94	20.3	8×10^4	800	6.0
0.85	1.71	56	6×10^6	7865	6.0
0.856	1.68	2×10^5	5×10^{10}	4×10^6	6.0
0.858	1.67	...	...	...	3.7
0.9	1.47	...	...	...	3.7
1.0	0.99				1.3
1.01	0.94		409	12	0.68
1.02	0.89		57	5	0.65

NOTE.—Ellipses indicate entries that could not be found numerically to exist.

they cannot obtain those solutions. We believe this result is real (and not an artifact of our scaling) since it is also observed in other analytical solutions (Tsinganos & Sauty 1993). It is also physically very interesting since, as we said, $x > 1$ solutions carry a nonzero axial electric current, and Appl & Camenzind (1992) have independently shown that current-carrying jets are stable!

We end the description of our solutions with a note on the fast magnetosonic critical point. Our numerical integration seems to indicate that there is a critical value of $x < 1$, above which the flow approaches (but never reaches) the fast magnetosonic point and never recollimates. In that case, we can explicitly obtain the asymptotic form of our equations (assuming that, as $Z \to \infty$, $R \to \infty$ and $R' \to 0$). The Bernoulli equation takes the form

$$\frac{1}{2} V_z^2 + \frac{\Omega_0^2}{F_0 V_z \epsilon} + \frac{H_0 \Omega_0}{F_0} = J_0 , \tag{47}$$

and the Grad-Shafranov equation becomes

$$\frac{Z\epsilon'}{\epsilon} = -(x-1)\left(1 - \frac{\Omega_0^2}{F_0 \epsilon V_z^3}\right), \tag{48}$$

where $\epsilon \equiv 1 - R'Z/R$. At these distances, the flow crosses the fast magnetosonic point when

$$V_z^3 = \frac{\Omega_0^2}{F_0 \epsilon} . \tag{49}$$

This gives

$$V_{zfms} = [\tfrac{2}{3}(J_0 - H_0 \Omega_0 / F_0)]^{1/2} , \tag{50}$$

$$\epsilon_{fms} = \frac{\Omega_0^2}{F_0 [2/3(J_0 - H_0 \Omega_0 / F_0)]^{3/2}} . \tag{51}$$

Equation (48) has the obvious solution $\epsilon = \text{const.}$, or equivalently,

$$R \propto Z^{1-\epsilon} , \tag{52}$$

in the special case when $x = 1$. The value of ϵ and the constant of proportionality are of course obtained only after we perform the detailed integration of equation (42) from $Z = 0$ and $R(0) = 1$ to infinity. We get a similar solution if the flow approaches asymptotically the fast magnetosonic point at infinity. In that case $\epsilon = \epsilon_{fms}$. As we said, the above asymptotic analysis is valid when $x_{crit} \le x \le 1$. When $x < x_{crit}$, the jet radius will eventually recollimate, whereas when $x > 1$, the jet radius oscillates around a finite value as $Z \to \infty$.

It is important to note that $\delta_0 \equiv v_K^2 / v_0^2$, the initial "gravity" parameter, plays a minor role in the asymptotic behavior of the solutions. However, δ_0 is an important parameter in detailed disk calculations of the origin of the jets, since at small axial distances away from the central compact object, gravity is important, and the larger δ_0, the larger the initial azimuthal magnetic field ($B_{\phi 0}/B_{z0} \approx H_0$) necessary to drive the flow to larger distances where gravity is unimportant (for very small values of $|H_0|$, no large-scale solutions exist).

The above results can be seen explicitly in Table 1 and Figure 2. We report in Table 1 the axial distance of the fast magnetosonic point ($Z_{fms} = z_{fms}/a_i$), the axial distance where the radius begins to recollimate ($Z_{max} = z_{max}/a_i$), and the radius and axial velocity at that distance ($R_{max} = r_{max}/a_i$ and $V_{zmax} = v_{zmax}/v_0$, respectively), for various values of x. These solutions have: $\delta_0 = 1$, $F_0 = 0.1$, $\Omega_0 = 1.18$, $H_0 = -1.89$, $J_0 = -1.66$, $\mathscr{K} = 0.01$, and $\Gamma = 5/3$. R'_0 is the initial slope required for each solution to cross the Alfvén singular point. In Figures 2*a*–2*c*, we plot the poloidal field-flow lines for the solutions with $x = 0.8$, $x = 0.9$, and $x = 1.02$, respectively. We see that when $x \le 0.856$, the flow crosses the fast magnetosonic point and eventually recollimates at a finite distance above the disk (Fig. 2*a*). The axial flow velocity attained at that distance is of the order of 5–10 times the initial rotational velocity at the base of the flow. When $0.856 < x < 1$, the flow does not cross the fast magnetosonic point and does not recollimate,

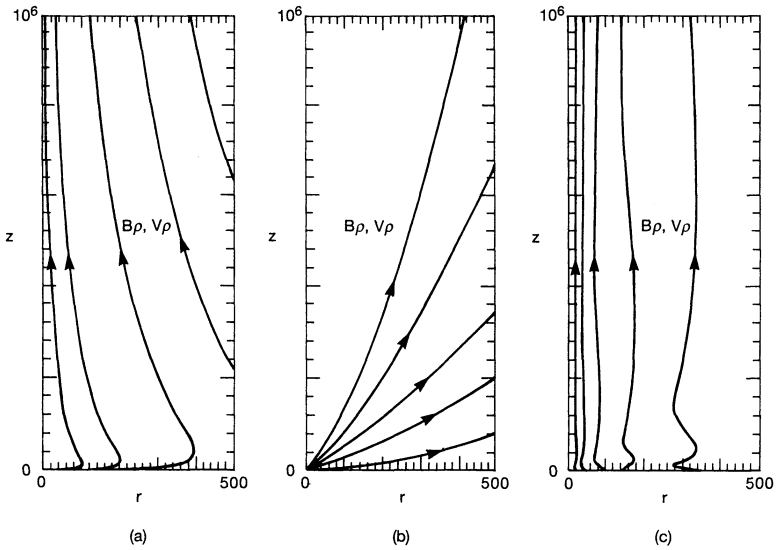

FIG. 2.—Representative outflow solutions for different values of the exponent x. $F_0 = 0.1$, $H_0 = -1.886$, $\delta_0 = 1$: (*a*) recollimating solution with $x = 0.8$; (*b*) nonrecollimating solution with $x = 0.9$; (*c*) oscillating solution with $x = 1.02$.

although we continued our integration to $Z \geq 10^{11}$ (Fig. 2*b*). However, $V_z \rightarrow V_{z\mathrm{fms}} = 3.7$ (eq. [50]). $x = 1$ is, as we saw before, a special solution of the equations. The solutions with $x > 1$ never cross the fast magnetosonic point and develop a series of radial oscillations (Fig. 2*c*).

4. THE BP LIMIT

We will finally compare our analysis to the BP limit, where $x = \frac{3}{4}$ and $\delta_0 = 1$ (Keplerian flow on the disk). The scaling of our quantities with radius on the disk is then: $v \propto r^{-1/2}$, $B \propto r^{x-2} \equiv r^{-5/4}$, $\rho \propto r^{2x-3} \equiv r^{-3/2}$, and $p \propto r^{2x-4} \equiv r^{-5/2}$, in accordance with BP's scaling. In the limit of zero pressure (cold MHD flow), BP start their integration from $V_z(0) = 0$. Therefore, equations (40) and (43) give us $J_0 = -3/2$ and $\Omega_0 = 1$.

Our notation follows the notation of LMMS; therefore, we need first to make the connection with BP's notation (listed on the left):

$$\begin{aligned} \chi &\leftrightarrow Z\,, \\ \xi(\chi) &\leftrightarrow R(Z)\,, \\ f(\chi) &\leftrightarrow V_z(Z)\,, \\ g(\chi) &\leftrightarrow V_\phi(Z)\,, \qquad \text{and} \\ (GM/r_0)^{1/2} &\leftrightarrow v_0\,. \end{aligned}$$

We can now easily make the connection between their and our dimensionless parameters:

$$\begin{aligned} \kappa &\leftrightarrow F_0\,, \\ \lambda &\leftrightarrow -H_0/F_0\,, \qquad \text{and} \\ \epsilon &\leftrightarrow J_0 - \Omega_0 H_0/F_0 = -3/2 + \lambda\,. \end{aligned}$$

BP also use the following notation:

$$\begin{aligned} J &\leftrightarrow R - ZR'\,, \\ T &\leftrightarrow R^2 + 2(R^2 + Z^2)^{-1/2} - 3\,, \\ U &\leftrightarrow 1 + (R')^2\,, \\ S &\leftrightarrow (R^2 + Z^2)^{-1/2}\,, \\ m &\leftrightarrow M_{\mathrm{Ap}}^2 \equiv F_0 V_z R(R - ZR')\,, \\ n &\leftrightarrow M_{\mathrm{A}}^2 \equiv M_{\mathrm{Ap}}^2 \frac{B_p^2}{B^2}\,, \qquad \text{and} \\ t &\leftrightarrow M_{\mathrm{A}}^2 \frac{(R - ZR')^2}{(1 + (R')^2)(R^2 + Z^2)}\,. \end{aligned} \tag{53}$$

TABLE 2

CHARACTERISTIC PARAMETERS OF THE BP SOLUTION: $F_0 = 0.03$, $-H_0/F_0 = 30$

Z	R	R'	V_p	V_ϕ	M_{Ap}	M_A
0	1	1.68	0	1	0	0
5.45	5.48	0.60	3.17	1.33	**1**	0.61
16.3	10.6	0.39	4.44	1.13	2.35	**1**
100	29.0	0.14	5.95	0.67	8.80	1.81
500	51.6	0.02	6.64	0.46	20.4	2.62
1246	57.3	**0**	6.87	0.44	26.0	3.12
5000	40.3	−0.005	7.13	0.67	23.7	4.20

We note here that m and n are simply the square of the Alfvén and fast magnetosonic Mach number, respectively (for a cold fluid). Now, equation (39) in BP notation gives $g = (\xi - \lambda m/\xi)/(1 - m)$, and equation (40) (the Bernoulli equation with $\Phi_g/v_0^2 = -(R^2 + Z^2)^{-1/2}$) gives:

$$\tfrac{1}{2} f^2 U + \tfrac{1}{2} g^2 - S - \xi g = -\tfrac{3}{2}\,, \tag{54}$$

which, together with the above equation for $g(\chi)$, yields equation (BP2.12) (we will use the prefix "BP" to refer to BP equation numbers). BP then consider the z-component of the Euler equation (eq. [5] without pressure), which combined with the component of the same equation parallel to the poloidal flow direction (which is just the differential form of the above Bernoulli equation), yields a second-order differential equation for $\xi(\chi)$ ($R(Z)$, eq. [BP2.17]). We instead consider the generalized Grad-Shafranov equation (this is just the component of the Euler equation along the direction perpendicular to the poloidal flow direction), again combined with the poloidal component of the same equation (eq. [41]), and we again get a second-order differential equation for $R(Z)$ (eq. [42]). The two approaches are, however, mathematically equivalent since any poloidal component of the Euler equation can be recovered from a linear combination of any two other poloidal components.

We check that equations (42) and (BP2.17) are indeed equivalent, by repeating BP's calculation for the special case $\kappa = 0.03$ and $\lambda = 30$. The parameters of our integration, according to the above discussion, are: $x = 3/4$, $\delta_0 = 1$ (initial Keplerian flow), $F_0 = 0.03$, $\Omega_0 = 1$, $H_0 = -0.9$, $J_0 = -3/2$, and $C_s = 0$ (no pressure). We begin the integration with $R(0) = 1$ and $V_z(0) = 0$. $R'(0)$ is specified by the condition that the flow goes smoothly through the Alfvén critical point. BP stop their integration at an arbitrary height $Z_{max} = 500$. We continue past that distance, and we show explicitly the radius recollimation ($R' < 0$). Table 2 displays the characteristics of the solution at the surface of the disk ($Z = 0$), the Alfvén critical point ($M_{Ap} = 1$), the fast magnetosonic point ($M_A = 1$), and the point where the radius begins to recollimate ($R' = 0$) (these three special points are indicated in boldface). There is reasonably good agreement between the entries in our table and those in BP's Table 1 (p. 896). BP's entries have small numerical errors, since they do not exactly satisfy the Bernoulli equation (BP2.10).

As a final check, we derive the BP limit of the asymptotic form of our equations as obtained in the previous section. In BP notation, equation (47) gives

$$\frac{1}{2} f^2 + \frac{1}{\kappa f (J/\xi)} - \lambda = -\frac{3}{2} \tag{55}$$

(eq. [BP2.25]), and equation (48) becomes

$$\chi\left(-\frac{\xi''\chi}{\xi} - \frac{\xi' J}{\xi^2}\right) = \frac{1}{4}\left(\frac{J}{\xi} - \frac{1}{\kappa f^3}\right) \tag{56}$$

(eq. [BP2.26]).

5. CONCLUSIONS

We have shown the existence of axisymmetric, time-independent, nonrelativistic, ideal, magnetohydrodynamic, collimated outflows from thin accretion disks around compact stars, with self-similar solutions of the full set of MHD equations which include matter flow, electromagnetic fields, pressure, and gravity. The parameters of the solutions are normalized to their respective values at the base of the flow (on the disk); hence, the same values of the dimensionless parameters apply to very different physical regimes.

The magnetic field accelerates the outflow perpendicular to the direction of the disk and provides collimation at large distances. The outflow velocities that we obtain are greater than or of the order of "a few times" the rotational velocity at the base of the flow (last column of Table 1). Therefore, the nonrelativistic treatment of the present work is relevant to small-scale stellar outflows from protostellar systems observed in our Galaxy. In order to describe extragalactic jets, which are thought to originate from the disk surrounding a black hole, we need to solve the relativistic equations presented in the Appendix. Solutions with relativistic terminal velocities have been obtained using the relativistic generalization of the method in LBC (Lovelace & Contopoulos 1992). The solution of the full set of relativistic equations is obtained in Contopoulos (1994).

The distribution of electric current flow along the jets is *the* important factor which regulates the general morphology of the outflow. The rotation of the disk drags the magnetic field lines and builds up a B_ϕ component with direction opposite to the direction of rotation (for $z > 0$). Therefore, the electric current that threads the jet downward within a radius r is $I = 2\pi c r B_\phi \propto r^{x-1}$.

When $x < 1$ (as in BP's solution), a singular current flows along the axis and the return (upward) current is distributed across the jet (the total current is zero; $I(r \to \infty) \to 0$). However, the electric current switches from infinite current density downward to infinite current density upward near the axis (in a physical situation we would expect this central downward-current region to have a finite radial extent). When $x \geq 1$, current flows downward across the jet. There is no return current in the solution; the circuit "closes" outside the jet, i.e., outside the region where our scaling is valid. We postulate that straight cylindrical jets are characterized by $x > 1$, i.e., by a nonzero electric current flowing along the jet. It is important to note again that Appl & Camenzind (1992) have independently shown that current-carrying configurations are more stable than non–current-carrying ones.

In order to calculate total mass, angular momentum, and energy flows along the jet, we need to truncate our self-similar solution with inner and outer physical cutoffs. We assume that the self-similar scalings are valid for $r_{\rm in}(z) \leq r \leq r_{\rm out}(z)$, with $r_{\rm in}(z = 0) = 0.1$ and $r_{\rm out}(z = 0) = 10$. This is an arbitrary (but convenient) choice that will only affect the values of the conserved quantities of the flow. Using the above expressions and reasonable values $\delta_0 \sim 1$, $x \sim 1$, the conserved quantities along each jet direction are (see LBC) the *mass-flow rate* in the jet across any $z = $ const. surface:

$$\dot{M} = \int_{z=\text{const.}} d^2x\, \rho v_z \sim 10^{-6}\, M_\odot\ \text{yr}^{-1}\, F_0 \left(\frac{a_i}{1\ \text{AU}}\right)^{5/2} \left(\frac{M}{1\ M_\odot}\right)^{-1/2} \left(\frac{B_0}{1\ \text{G}}\right)^2 = \text{const.}\,, \tag{57}$$

the *angular momentum* about the z-axis *flow rate*:

$$\dot{L}_z = \int_{z=\text{const.}} d^2x\, r(\rho v_z v_\phi - B_z B_\phi/4\pi) \sim 10^{-4}\, M_\odot(\text{km s}^{-1})\text{AU yr}^{-1}\, (-H_0) \left(\frac{a_i}{1\ \text{AU}}\right)^3 \left(\frac{B_0}{1\ \text{G}}\right)^2 = \text{const.}\,, \tag{58}$$

and the *energy flow rate*:

$$\dot{E} = \int_{z=\text{const.}} d^2x\, \rho v_z \left[\frac{1}{2} v_r^2 + \frac{1}{2}(r\omega)^2 + \frac{1}{2} v_z^2 + w + \Phi_g\right] + \frac{c}{4\pi} \int_{z=\text{const.}} d^2x\, E_r B_\phi$$

$$\sim 1\ L_\odot\ F_0 \left(J_0 - \frac{\Omega_0 H_0}{F_0}\right) \left(\frac{a_i}{1\ \text{AU}}\right)^{3/2} \left(\frac{M}{M_\odot}\right)^{1/2} \left(\frac{B_0}{1\ \text{G}}\right)^2 = \text{const.}\,, \tag{59}$$

where $\rho v_i(|\boldsymbol{v}|^2/2 + w + \Phi_g)$ is the energy flux density carried by the fluid (w is the enthalpy per unit mass), $(c/4\pi)\,(\boldsymbol{E} \times \boldsymbol{B})_i$ is the Poynting energy flux carried by the electromagnetic field, and Φ_g is the gravitational potential. Note that in order to take into account the two symmetric jet directions $\pm z$, we need to multiply the above effluxes by a factor of 2. These expressions can apply to both galactic and extragalactic outflows. For example, for typical values $F_0 = 0.3$, $H_0 = -5$, $\Omega_0 = 1$, and $J_0 = -1.5$, we get $\dot{M} \sim 10^{-7}\, M_\odot\ \text{yr}^{-1}$ and $\dot{E} \sim 10\, L_\odot$, for an $M \sim 1\, M_\odot$, $a_i \sim 10^{-2}$ AU, and $B_0 \sim 10^2$ G young stellar object and we get $\dot{M} \sim 10^{-1}\, M_\odot\ \text{yr}^{-1}$ and $\dot{E} \sim 10^{13}\, L_\odot$, for an $M \sim 10^8\, M_\odot$, $a_i \sim 1$ AU, and $B_0 \sim 10^4$ G extragalactic outflow.

We finally note that the magnetic field can be a very efficient factor in removing angular momentum from the disk. An estimate of the timescale for accretion gives

$$T_{\rm accr} \sim \frac{(L_z)_{\rm disk}}{(\dot{L}_z)_{\rm jet}} \sim \left(\frac{\rho_{\rm disk} v_0^2}{B_z B_\phi}\right) \left(\frac{h}{R}\right) T_{\rm rot}\,, \tag{60}$$

where h/R is the ratio of height to radius of the disk and $T_{\rm rot}$ is the rotational period. We see that if we assume energy equipartition between the disk rotation and the magnetic field (which is reasonable if the disk is sufficiently ionized), then even for a not-so-thin disk, the timescale for accretion can be comparable to the rotational period. The magnetic field can then be dynamically important in regulating the accretion.

We thank Demosthenes Kazanas for discussions and encouragement. This work was supported in part by NASA grant NAGW 2293 from the Origins of the Solar System Program.

APPENDIX

We consider here the more general case of *relativistic* axisymmetric magnetohydrodynamic flows for the case of a weak gravitational field ($|\Phi_g|/c^2 \ll 1$) and negligible pressure. This approximation of relativistic and "cold" outflows is reasonable at large distances away from the central object.

Following Lovelace et al. (1986) for the special relativistic limit where gravity and gas pressure are negligible, we obtain the relativistically generalized Grad-Shafranov equation:

$$\left(1 - \frac{r^2\Omega^2}{c^2} - \frac{\gamma F^2}{4\pi\rho}\right)\Delta^*\Psi - \frac{1}{2r^2}\nabla\left(\frac{r^4\Omega^2}{c^2}\right)\cdot\nabla\Psi - F\nabla\left(\frac{\gamma F}{4\pi\rho}\right)\cdot\nabla\Psi = -(H + \gamma r v_\phi F)(H' + \gamma r v_\phi F') - 4\pi\rho r^2(J' + \gamma r v_\phi \Omega')\,, \tag{A1}$$

where again $(\cdot)' \equiv d(\cdot)/d\Psi$, $\gamma \equiv (1 - |\boldsymbol{v}|^2/c^2)^{-1/2}$ is the Lorentz factor of the flow, $\rho \equiv \gamma n \mu$ is an effective mass density in the laboratory reference frame, and the four arbitrary functions F, Ω, H, and J of Ψ enter through the following four relations:

$$F(\Psi) = 4\pi\rho \frac{|\boldsymbol{v}_p|}{|\boldsymbol{B}_p|}, \tag{A2}$$

$$\Omega(\Psi) = \frac{1}{r}\left(v_\phi - \frac{F(\Psi)}{4\pi\rho} B_\phi\right), \tag{A3}$$

$$H(\Psi) = rB_\phi - \gamma F(\Psi) r v_\phi, \tag{A4}$$

$$1 + \frac{J(\Psi)}{c^2} = \gamma\left(1 - \frac{\Omega(\Psi) r v_\phi}{c^2}\right). \tag{A5}$$

Equation (A5) is the generalized Bernoulli equation. The notation is the same as in § 2. We consider again the same simple form for the equation of a field-flow line,

$$r = r_\Psi(z) = r_\Psi R(z/r_\Psi) \equiv r_\Psi R(Z). \tag{A6}$$

Here r and z are dimensionless as before, rescaled to the "characteristic" radius a_i. Using the generalized Euler equation, the following expressions enable us once more to rescale the r_Ψ terms in the relativistic MHD equations:

$$\Psi(r, z) = (r_\Psi)^x \Psi_0, \tag{A7}$$

$$\boldsymbol{B}(r, z) = (r_\Psi)^{x-2} \boldsymbol{B}(Z), \tag{A8}$$

$$\boldsymbol{v}(r, z) = \boldsymbol{V}(Z) v_0, \tag{A9}$$

$$\rho(r, z) = (r_\Psi)^{2x-4} \rho(Z) \frac{B_0^2}{v_0^2}, \tag{A10}$$

$$F(\Psi) = (r_\Psi)^{x-2} F_0 \frac{B_0}{v_0}, \tag{A11}$$

$$\Omega(\Psi) = (r_\Psi)^{-1} \Omega_0 \frac{v_0}{a_i}, \tag{A12}$$

$$H(\Psi) = (r_\Psi)^{x-1} H_0 a_i B_0, \qquad \text{and} \tag{A13}$$

$$J(\Psi) = J_0 v_0^2, \tag{A14}$$

where $\boldsymbol{V}, \rho, F_0, \Omega_0, H_0$, and J_0 are again dimensionless. Note that in the nonrelativistic case the scaling of $\boldsymbol{v}$ came out of the gravitational potential scaling. Here the neglect of the gravity terms is very helpful because any scaling of $\boldsymbol{v}$ with r_Ψ would be a problem in the $\gamma = (1 - |\boldsymbol{v}|^2/c^2)^{-1/2}$ terms. Now $\gamma(r, z) = (1 - |\boldsymbol{V}(Z)|^2/c_n^2)^{-1/2} \equiv \gamma(Z)$. Note also that velocities are again normalized to the initial rotational velocity v_0, and not to the speed of light c, in order to make the connection with the expressions of § 2. The expressions for $(r_\Psi)_r$, $(r_\Psi)_z$, Z_r, Z_z, $(r_\psi)_{rr}$, and $(r_\Psi)_{zz}$ are the same as before (eqs. [28]–[33]). Using the above expressions and factoring out $(r_\Psi)^{x-2} B_0$, the generalized Grad-Shafranov equation takes the form

$$\left[1 - \frac{R^2\Omega_0^2}{c_n^2} - \gamma F_0 V_z R(R - ZR')\right]\left[-\frac{1}{R(R - ZR')} + (x - 1)\frac{1 + (R')^2}{(R - ZR')^2} - R''\frac{R^2 + Z^2}{(R - ZR')^3}\right]$$
$$- \frac{\Omega_0^2}{c_n^2}\left[\frac{2R}{R - ZR'} - R^2\frac{1 + (R')^2}{(R - ZR')^2}\right] + F_0 \frac{1}{R - ZR'}\left[(Z + RR')\left(\gamma' V_z R + \gamma V_z' R + \gamma V_z R' - \gamma V_z R \frac{ZR''}{R - ZR'}\right)\right.$$
$$\left. + \gamma V_z R(x - 2)(1 + (R')^2)\right] = -(H_0 + \gamma R V_\phi F_0)[(x - 1)H_0 + \gamma R V_\phi (x - 2)F_0] + \gamma F_0 \frac{\Omega_0 R^2 V_\phi}{V_z(R - ZR')}, \tag{A15}$$

and the generalized Bernoulli equation the form

$$\gamma\left(1 - \frac{R\Omega_0 V_\phi}{c_n^2}\right) = 1 + \frac{J_0}{c_n^2}. \tag{A16}$$

This is the equation that we have to root-solve numerically to obtain V_z as a function of R, R', and Z. We also have that

$$V_\phi = \frac{R\Omega_0 + H_0 V_z(R - ZR')}{1 - \gamma F_0 V_z R(R - ZR')}. \tag{A17}$$

We now differentiate the Bernoulli equation with respect to Z, and after some algebra, we obtain:

$$V_z' = \mathcal{I} + R''\mathcal{J}, \tag{A18}$$

where

$$\mathcal{I}(R, R', Z) = \frac{(\gamma R\Omega_0/c_n^2)(\mathcal{A} + \mathcal{E}\mathcal{F}) - \mathcal{F}[1 - (R\Omega_0 V_\phi/c_n^2)] + (\gamma R'\Omega_0 V_\phi/c_n^2)}{\mathcal{G}[(1 - (R\Omega_0 V_\phi/c_n^2)] - (\gamma R\Omega_0/c_n^2)(\mathcal{B} + \mathcal{E}\mathcal{G})},$$

$$\mathcal{J}(R, R', Z) = \frac{(\gamma R\Omega_0/c_n^2)(\mathcal{C} + \mathcal{E}\mathcal{H}) - \mathcal{H}[1 - (R\Omega_0 V_\phi/c_n^2)]}{\mathcal{G}[1 - (R\Omega_0 V_\phi/c_n^2)] - (\gamma R\Omega_0/c_n^2)(\mathcal{B} + \mathcal{E}\mathcal{G})},$$

and

$$\mathcal{A}(R, R', Z) = \frac{R'\Omega_0 + \gamma F_0 V_\phi V_z R'(R - ZR')}{1 - \gamma F_0 V_z R(R - ZR')},$$

$$\mathcal{B}(R, R', Z) = \frac{H_0(R - ZR') + \gamma F_0 V_\phi R(R - ZR')}{1 - \gamma F_0 V_z R(R - ZR')},$$

$$\mathcal{C}(R, R', Z) = \frac{-H_0 V_z Z - \gamma F_0 V_z RZV_\phi}{1 - \gamma F_0 V_z R(R - ZR')},$$

$$\mathcal{E}(R, R', Z) = \frac{F_0 V_\phi V_z R(R - ZR')}{1 - \gamma F_0 V_z R(R - ZR')},$$

$$\mathcal{F}(R, R', Z) = \frac{\gamma^3}{c_n^2}\frac{V_\phi \mathcal{A}}{1 - (\gamma^3/c_n^2)V_\phi \mathcal{E}},$$

$$\mathcal{G}(R, R', Z) = \frac{\gamma^3}{c_n^2}\frac{V_z(1 + (R')^2) + V_\phi \mathcal{B}}{1 - (\gamma^3/c_n^2)V_\phi \mathcal{E}},$$

$$\mathcal{H}(R, R', Z) = \frac{\gamma^3}{c_n^2}\frac{V_z^2 R' + V_\phi \mathcal{C}}{1 - (\gamma^3/c_n^2)V_\phi \mathcal{E}}.$$

The above forms come in the expressions

$$V'_\phi = \mathcal{A} + V'_z \mathcal{B} + R''\mathcal{C} + \gamma'\mathcal{E}, \tag{A19}$$

$$\gamma' = \mathcal{F} + V'_z \mathcal{G} + R''\mathcal{H} = \mathcal{K} + R''\mathcal{L}, \tag{A20}$$

where

$$\mathcal{K}(R, R', Z) \equiv \mathcal{F} + \mathcal{I}\mathcal{G},$$

$$\mathcal{L}(R, R', Z) \equiv \mathcal{J}\mathcal{G} + \mathcal{H}.$$

Finally, going back to the generalized Grad-Shafranov equation and putting everything back, we obtain

$$\left[1 - \frac{R^2\Omega_0^2}{c_n^2} - \gamma F_0 V_z R(R - ZR')\right]\left[-\frac{1}{R(R - ZR')} + (x - 1)\frac{1 + (R')^2}{(R - ZR')^2} - R''\frac{R^2 + Z^2}{(R - ZR')^3}\right]$$
$$- \frac{\Omega_0^2}{c_n^2}\frac{-2RR'Z + R^2(1 - (R')^2)}{(R - ZR')^2} + F_0\frac{1}{R - ZR'}\left[(Z + RR')(\gamma V_z R' + V_z R\mathcal{K} + \gamma R\mathcal{I}) + \gamma V_z R(x - 2)(1 + (R')^2)\right.$$
$$\left. + (Z + RR')\left(V_z R\mathcal{L} + \gamma R\mathcal{J} - \frac{\gamma V_z RZ}{R - ZR'}\right)R''\right]$$
$$= -(H_0 + \gamma RV_\phi F_0)[(x - 1)H_0 + \gamma RV_\phi(x - 2)F_0] + \gamma F_0\frac{\Omega_0 R^2 V_\phi}{V_z(R - ZR')}, \tag{A21}$$

which gives the final equation

$$R'' = \frac{\mathcal{M}}{\mathcal{N}}(R, R', Z), \tag{A22}$$

where

$$\mathcal{N}(R, R', Z) = \left[1 - \frac{R^2\Omega_0^2}{c_n^2} - \gamma F_0 V_z R(R - ZR')\right]\left[-\frac{R^2 + Z^2}{(R - ZR')^3}\right] + F_0\frac{1}{R - ZR'}(Z + RR')\left(V_z R\mathcal{L} + \gamma R\mathcal{J} - \frac{\gamma V_z RZ}{R - ZR'}\right),$$

and

$$\mathcal{M}(R, R', Z) = -(H_0 + \gamma F_0 R V_\phi)[(x-1)H_0 + \gamma F_0 (x-2) R V_\phi] + \gamma F_0 \Omega_0 \frac{R^2 V_\phi}{V_z (R - ZR')}$$
$$- \left[1 - \frac{R^2 \Omega_0^2}{c_n^2} - \gamma F_0 V_z R (R - ZR')\right]\left[-\frac{1}{R(R-ZR')} + (x-1)\frac{1 + (R')^2}{(R-ZR')^2}\right] + \frac{\Omega_0^2}{c_n^2}\frac{-2RR'Z + R^2(1-(R')^2)}{(R-ZR')^2}$$
$$- F_0 \frac{1}{R - ZR'}[(Z + RR')(\gamma V_z R' + V_z R\mathcal{K} + \gamma R\mathcal{J}) + \gamma V_z R(x-2)(1 + (R')^2)] .$$

This is the final second-order ordinary differential equation for $R(Z)$, which can be integrated numerically. The solution for the flow and the fields in the entire poloidal r-z plane is obtained as before through equations (A6)–(A10).

REFERENCES

Appl, S., & Camenzind, M. 1992, A&A, 256, 354
Bally, J., Langer, W. D., Stark, A. A., & Wilson, R. W. 1987, ApJ, 312, L45
Begelman, M. C., Blandford, R. D., & Rees, M. J. 1984, Rev. Mod. Phys., 56, 255
Blandford, R. D., & Payne, D. G. 1982, MNRAS, 199, 883 (BP)
Camenzind, M. 1987, A&A, 184, 341
Chan, K. L., & Henriksen, R. N. 1980, ApJ, 241, 534
Contopoulos, J. 1994, ApJ, in press
Heinemann, M., & Olbert, S. 1978, J. Geophys. Res., 83, 2457
Hughes, P. A. 1991, Beams and Jets in Astrophysics (Cambridge: Cambridge Univ. Press)
Hughes, P. A., Aller, H. D., & Aller, M. F. 1985, ApJ, 298, 301
———. 1989a, ApJ, 341, 54
———. 1989b, ApJ, 341, 68
Jackson, J. D. 1975, Classical Electrodynamics (2d ed.; New York: Wiley)
Königl, A. 1989, ApJ, 342, 208
Koupelis, T., & Van Horn, H. M. 1989, ApJ, 342, 146
Lovelace, R. V. E., Berk, H. L., & Contopoulos, J. 1991, ApJ, 379, 696 (LBC)
Lovelace, R. V. E., & Contopoulos, J. 1992, in Ann. NY Acad. Sci. No. 675, 7th Florida Workshop on Nonlinear Astronomy: Astrophysical Disks, ed. S. F. Dermott et al., 286
Lovelace, R. V. E., Mehanian, C., Mobarry, C. M., & Sulkanen, M. E. 1986, ApJS, 62, 1 (LMMS)
Lovelace, R. V. ., Wang, J. C. L., & Sulkanen, M. E. 1987, ApJ, 315, 504
Mouschovias, T. Ch., & Paleologou, E. V. 1980, Moon & Planets, 22, 31
Mundt, R., Ray, T. P., & Raga, A. C. 1991, A&A, 252, 740
Parker, E. N. 1963, Interplanetary Dynamical Processes (New York: Wiley)
Pudritz, R. E. 1985, ApJ, 293, 216
———. 1988, in Galactic and Extragalactic Star Formation, ed. R. E. Pudritz & M. Fich (Dordrecht: Kluwer), 135
Sakurai, T. 1985, A&A, 152, 121
Tsinganos, K., & Sauty, C. 1993, in Proc. 1st Panhellenic Astronomical Meeting, ed. P. G. Lascarides (Athens: National Committee for Astronomy), 391
Tsinganos, K., & Trussoni, E. 1990, A&A, 231, 270
Ungerechts, H., & Thaddeus, P. 1987, ApJS, 63, 645
Wang, J. C. L., Sulkanen, M. E., & Lovelace, R. V. E. 1992, ApJ, 390, 46
Wardle, J. F. C., & Roberts, D. H. 1988, in The Impact of VLBI on Astrophysics and Geophysics, ed. M. J. Reid & J. M. Moran (Dordrecht: Kluwer), 143
Weber, E. J., & Davis, L., Jr. 1967, ApJ, 148, 217